

1
2 Urbanization Dramatically Altered the Water Balances of a Paddy Field Dominated Basin in
3 Southern China

4 Lu Hao¹, Ge Sun^{2*}, Yongqiang Liu³, Jinhong Wan⁴, Mengsheng Qin¹, Hong Qian¹, Chong Liu⁵,
5 Jiangkun Zheng⁶, Ranjeet John⁷, Peilei Fan⁸, and Jiquan Chen⁷

6
7 1. International Center for Ecology, Meteorology, and Environment (IceMe), Jiangsu Key
8 Laboratory of Agricultural Meteorology, Nanjing University of Information Science and
9 Technology (NUIST), Nanjing 210044, China.

10 2. ***Ge Sun (Corresponding Author)**, Research Hydrologist, Eastern Forest Environmental
11 Threat Assessment Center, Southern Research Station, USDA Forest Service, Raleigh, NC
12 27606, USA. Email: gesun@fs.fed.us; Phone: (919)5159498 (O), Fax: (919)5132978

13 3. Center for Forest Disturbance Science, Southern Research Station, USDA Forest Service,
14 Athens, GA 30602, USA

15 4. China Institute of Water Resources and Hydropower Research, Beijing 100048, China.

16 5. State Key Laboratory for Information Engineering in Surveying, Mapping and Remote
17 Sensing, Wuhan University, Wuhan 430079, China.

18 6. College of Forestry, Sichuan Agricultural University, Ya'an, Sichuan, China

19 7. Center for Global Change and Earth Observations (CGCEO), and Department of
20 Geography, Michigan State University, East Lansing, MI 48823, USA.

21 8. School of Planning, Design, and Construction (SPDC) and Center for Global Change and
22 Earth Observations (CGCEO), Michigan State University, East Lansing, MI 48823, USA.
23

24 **Abstract.** Rice paddy fields provide important ecosystem services (e.g., food production, water
25 retention, carbon sequestration) to a large population globally. However, these benefits are
26 diminishing as a result of rapid environmental and socioeconomic transformations characterized by
27 population growth, urbanization, and climate change in many Asian countries. This case study
28 examined the responses of streamflow and watershed water balances to the decline of rice paddy
29 fields due to urbanization in the Qinhuai River Basin in southern China where massive
30 industrialization has occurred during the past three decades. We found that streamflow increased
31 by 58% and evapotranspiration (ET) decreased by 23% during 1986-2013 as a result of an increase
32 in urban areas of three folds and reduction of rice paddy field by 27%. Both highflows and
33 lowflows increased significantly by about 28% from 2002 to 2013. The increases in streamflow
34 were consistent with the decreases in ET and leaf area index monitored by independent remote
35 sensing MODIS data. Attribution analysis based on two empirical models indicted that land
36 use/land cover change contributed about 82-108% of the observed increase in streamflow from
37 353 ± 287 mm yr⁻¹ during 1986-2002 to 556 ± 145 during 2003-2013. We concluded that the
38 reduction in ET was largely attributed to the cropland conversion to urban use. The effects of land
39 use change overwhelmed the effects of regional climate warming and climate variability.
40 Converting traditional rice paddy fields to urban use dramatically altered land surface conditions
41 from an artificial wetland-dominated landscape to an urban land use- dominated one, and thus was
42 considered as one of the extreme types of contemporary hydrologic disturbances. The ongoing
43 large-scale urbanization in the rice paddy-dominated regions in the humid southern China, and
44 East Asia, will likely elevate stormflow volume, aggravate flood risks, and intensify urban heat
45 island effects. Understanding the linkage between land use/land cover change and changes in

46 hydrological processes is essential for better management of urbanizing watersheds in the rice
47 paddy dominated landscape.

48 **1 Introduction**

49 Urbanization is a global phenomenon that poses profound threats to the local environment,
50 society, and culture (Foley et al., 2005; McDonald et al., 2011). The most obvious direct
51 consequence of urbanization is the altered hydrology and water balances that control the flows of
52 energy and matter in watershed ecosystems (Paul and Meyer, 2001; Sun and Lockaby, 2012). In
53 addition to the direct hydrologic impacts, indirect impacts of urbanization on local weather
54 patterns (e.g., rainfall intensity and surface air temperature) were also becoming increasingly
55 important under a changing climate (Yang et al., 2013).

56 It is widely known that urbanization elevates peakflow rates (Brath et al., 2006; Du et al.,
57 2012; Sun and Lockaby, 2012) as a result of increased impervious surfaces that promote quick
58 surface runoff (Dietz and Clausen, 2008; Miller et al., 2014). However, the hydrologic response
59 to urbanization is extremely variable (Jacobson, 2011; Caldwell et al., 2012) due to climatic
60 differences and land use change patterns across a watershed (Sun and Lockaby, 2012). Empirical
61 data are still lacking about changes in water balances and watershed hydrologic characteristics
62 other than stormflow, such as total flow, lowflow, and evapotranspiration (ET) (Dow and
63 DeWalle, 2000; Boggs and Sun, 2011) in different physiographic settings (Barron et al., 2013).
64 Previous studies rely heavily on simulation models (Kang et al., 1998; Kim et al., 2005, 2014;
65 Sakaguchi et al., 2014). Controversies on the magnitude and underlying mechanisms of

66 hydrologic responses to land conversion during urbanization remain in the literature (Wang et al.,
67 2009; He et al., 2009; Sun and Lockaby, 2012). In particular, data are scarce on the effects of
68 converting paddy fields to other land uses, resulting in conflicting conclusions. For example, a
69 simulation study in Taiwan suggested that rice paddy fields generated 55% lower total runoff
70 and 33% lower peakflows than dry farms (Wu et al., 1997). However, another simulation study
71 that used the HEC-HMS model for a rice paddy dominated watershed in southern China found
72 that an increase in impervious surface areas from 3% to 30% increased the peakflow rate and
73 storm volume (4-20%), but had very limited impacts on total annual flow (<6%) (Wang et al.,
74 2009; Du et al., 2011, 2012) and thus long term water balances.

75 The highly populated Yangtze River Delta (YRD) region covers about 2% of China's land
76 mass, but provides over 18% of China's Gross Domestic Product (Gu et al., 2011). The population
77 increased by almost 13% in the past decade to 156 million in 2013, and has become China's most
78 industrialized region and one of the global 'hot spots' of economic and social development. As the
79 'homes of the fish and rice', southern China's landscapes have been dominated by rice paddy
80 fields for thousands of years. The original coastal wetlands have long been ditched, drained, and
81 cultivated for growing rice and other crops. Rice paddy fields are major sources of food
82 production and offer many other ecosystem services similar to wetlands including flood retention,
83 groundwater recharge (He et al., 2009), nutrient cycling, and sequestration of greenhouse gases
84 (Tsai, 2002). One study on 10 typical rice paddies in China concluded that their ecosystem service
85 values exceed their economic values by three folds (Xiao et al., 2011). The rapid urbanization and
86 population rise under a warming climate in the YRD region has caused serious environmental and
87 resource concerns such as overdrawing and pollution of groundwater, flooding, land subsidence,

88 and urban heat islands (He et al., 2007; Gu et al., 2011; Zhao et al., 2014). The majority of the
89 existing studies on paddy fields have focused on grain yield and irrigation with little research on
90 the hydrologic response to urbanization in paddy field-dominated landscapes (Du et al., 2011,
91 2012; Kim et al., 2014).

92 Converting paddies to urban land use have many cascading effects on the local environments
93 (Figure 1). In particular, because rice paddy fields are rarely under water stress, the water loss or
94 actual ET is close to the potential ET (Wu et al., 1997) and has been recognized as their cooling
95 functions in regulating local climate (Xiao et al., 2011). In contrast, urban land use is generally
96 characterized by low vegetation coverage with low ET and high runoff (Sun and Lockaby, 2012).
97 A study on China's 32 cities by Zhou et al. (2014) concluded that UHI effects dropped more
98 sharply from urban centers to the rural areas in the humid southern China than in northern China
99 or inland cities, indicating the stronger contrast of energy regime in the paddy-dominated regions
100 than that in other regions.

101 Therefore, we hypothesized that converting rice paddy fields to urban areas represents the
102 maximum ET reduction possible among all common land cover change scenarios, potentially
103 resulting in disproportionately higher impacts on water balances than other land conversion
104 scenarios (e.g., converting dryland to urban uses) . Along with the increase in impervious surface
105 areas that are well known to increase stormflow, ET reduction during urbanization is likely to
106 cause large impacts on the local micro-climate, streamflow, and water quality on paddy field
107 dominated watersheds (Figure 1).

108 The overall goal of this study was to understand the processes underlining the hydrologic
109 impacts of converting rice paddy fields to urban uses. The specific objectives of this study were: 1)

110 examine how urbanization in the past decade (2000-2013) has affected the water balances and
111 hydrologic characteristics of the Qinhuai River Basin (QRB), a typical landscape of the YRD
112 (Figure 2), 2) test the hypothesis that urbanization in a paddy field dominated watershed
113 dramatically reduced ET, thus altered water balances, and 3) explore the implications of
114 urbanization for regional environmental change in southern China. In this study, we integrated
115 long-term hydro-meteorological monitoring data and remote sensing-based ET and vegetation
116 products. Multiple advanced detection techniques were used to examine trends of climate and
117 streamflow overtime and their associations with biophysical variables such as leaf area index and
118 land use dynamics.

119 **2 Methods**

120 **2.1 The Qinhuai River Basin (QRB)**

121 As one of the tributaries of the Yangtze River, the QRB (31°34′-32°10′N, 118°39′-119°19′E) has
122 a catchment area of 2,617 km². The QRB represents a typical landscape of the lower Yangtze
123 River Delta region that is characterized as having a flat topography with natural river networks
124 severely modified, and the land uses were dominated by paddy rice fields dotted with small
125 irrigation ponds that were converted from natural wetlands over thousands of years (Figure 2). As
126 the ‘Backyard Garden’ of Nanjing City, Capital of Jiangsu Province, the QRB is gradually
127 recognized for its important ecosystem services in drought/flood prevention, crop irrigation,
128 recreation, tourism, and emergency drinking water supply to over 8 million residents. The local
129 climate is controlled by the East Asia summer monsoon (Guo et al., 2012). The multi-year mean
130 air temperature is 15.4°C. Mean air temperature (1961-2013) across the study basin has increased
131 drastically at rate of 0.44 °C/decade from 1990 to 2013 (Figure 3), suggesting an increasing trend

132 in evaporative potential during the past two decades. The mean (1986-2013) annual precipitation
133 is 1,116 mm with 75% rainfall falling during April-October (Figure 4). The observed long-term
134 mean annual streamflow (per unit of area) is about 430 mm, concentrated from June to August.
135 The QRB has seen rapid urbanization during the past decade. The urban built-up areas increased
136 from 9% (222km²) to 12% (301 km²) from 2000 to 2004, but jumped to 23% (612 km²) in 2012,
137 and the area of rice paddy fields decreased from 45% (1,188km²) of the total land area in 2000 to
138 43% (1,112 km²) in 2004, and dramatically dropped to 36% (932 km²) in 2012 (Figure 2).
139 Documents by Jiangsu Province Rural Statistics reported that rice planting area in the QRB shrank
140 more than 25% from 995 km² in 2000 to 745 km² in 2010.

141 **2.2 Land use, Climate, Streamflow, Potential ET, ET, and Leaf Area Index (LAI)**

142 We retrieved land use and land cover (LULC) data for four key time periods, 2000, 2004, 2007
143 and 2012, using Landsat TM and ETM+ images with a 30 m pixel resolution
144 (<http://glovis.usgs.gov/>). We also compared our analysis to land use and land cover data acquired
145 for the period from 1988 to 2012 from other multiple sources, including published thesis and
146 journal papers for the study basin (Du et al., 2012; Chen and Du, 2014). For land use in 2010, we
147 also used the new Finer Resolution Observation and Monitoring of Global Land Cover that was
148 created by Tsinghua University using Landsat TM and ETM+ data (Gong et al., 2013). The daily
149 meteorological data (Precipitation, Radiation, Temperature, Wind Speed, and Humidity) for
150 estimating potential ET were acquired from four standard climatic stations maintained by the local
151 meteorological bureau across the QRB (Figure 2). Streamflow data with varying temporal
152 resolutions were compiled from hydrologic records for two hydrological stations, the Wuding

153 Sluice Gate (Wuding Station thereafter) and the Inner Qinhuai Sluice Gate (Inner Qinhuai Station
154 thereafter), which controlled the outflows from the Qinhuai River and backflows from the Yangtze
155 River (Figure 2). The daily streamflow data (2002-2003; 2006-2013) for the ‘flooding periods’
156 from May to October recorded at the Wuding Station were used to characterize highflows and
157 lowflows. The total annual streamflow discharged to the Yangtze River was the sum of flows
158 measured at the Wuding Station and the Inner Qinhuai Station. Total annual streamflow data for
159 the period of 1986-2006 were reported in Du et al. (2011) and we collected daily and monthly
160 streamflow data for other periods (Table 1).

161 Potential ET (PET) represents the maximum ecosystem evapotranspiration when soil water is
162 not limited, such as the case of paddy fields. PET represents a comprehensive index of availability
163 of atmospheric evaporative energy that is controlled by radiation, temperature, humidity, and wind
164 speed. Daily PET rates were calculated using the standard FAO 56 method and were averaged
165 across the four climatic stations for the period 2000-2013 (Allen et al., 1994). The improved
166 MOD16 datasets provide consistent estimates of global actual ET at an eight-day and 1-km²
167 resolution (Mu et al., 2011). Yuan et al. (2011) reprocessed the MODIS leaf areas index (LAI)
168 datasets using the modified temporal spatial filter (mTSF) and time-series analysis with the
169 TIMESAT software (Jonsson and Eklundh, 2004) and provided reliable continuous LAI estimates
170 from 2000 to 2013. Mean monthly PET and MODIS ET rates were presented in Figure 4 along
171 with other climatic variables to contrast seasonal ET, PET, and P that controlled seasonal
172 streamflow.

173 **2.3 Change Detection**

174 Three statistical methods were used to comprehensively examine the temporal changes in the

175 long-term hydro-climatic data series: (1) The Mann-Kendall test (Mann, 1945; Kendall, 1975) for
176 the non-linear trend at significance levels of $\alpha = 0.001, 0.01, 0.05,$ and $0.10,$ (2) The Sen's
177 nonparametric method was applied to examine the linear trend and to estimate the true slope of an
178 existing trend as change per year (Gilbert, 1987), and (3) The Dynamic Harmonic Regression
179 (DHR) method used for determining the change rates for meteorological, hydrological, and LAI
180 time series based on the Captain Toolbox (Taylor et al., 2007). The DHR model was used to fit
181 three main components in a time series including the trend of the original time series, the
182 periodicity, and the residuals, which were referred as Gaussian white noise for convenience. The
183 key feature of the DHR model is its ability to characterize the seasonal or periodic components of
184 time series data, so the method is suitable for analyzing time series with remarkable seasonal
185 variations. The DHR model analyzes the seasonal or periodic component using a similar approach
186 as Fourier analysis.

187 We used a series of common hydrologic detection methods to determine magnitude and
188 timing of the effects of land use change and climate change on streamflow (Ma et al., 2010; Tang
189 et al., 2011; Wei and Zhang, 2012). The Flow Duration Curve (FDC) (Vogel and Fennessey, 1993)
190 and the Double Mass Curve (DMC) methods (Wei and Zhang, 2010) were used to determine
191 changes of streamflow frequency in daily and annual streamflow as a result of urbanization,
192 respectively.

193 The trend of the baseflow component of the streamflow is one important indicator of change
194 in soil water storage, i.e., soil moisture and groundwater conditions (Price et al., 2011). The
195 Baseflow Index (BFI) program was used to separate the baseflow from measured total daily
196 streamflow (Wahl and Wahl, 1995). Our results showed that $N,$ the number of days over which a

197 minimum flow could be determined, was 7 days for the study basin (Figure 5), suggesting that BFI
 198 (baseflow/streamflow ratio) would not change much shorter than 7 days. We used a value of 0.9
 199 for the turning point factor (f) to remove daily streamflow greater than $100 \text{ m}^3 \text{ s}^{-1}$. Details of the
 200 methods to determine N and f can be found in Wahl and Wahl (1995).

201 **2.4 Attribution Analysis**

202 Once hydrologic change point was detected, we determined the individual contributions of climate
 203 and landcover/land use change to the observed streamflow change. We assumed that the observed
 204 streamflow change (ΔQ) in the study basin could be explained by the sum of change in climate
 205 (ΔQ_{clim}) and change in land use/land cover (i.e., urbanization) (ΔQ_{lulc}):

$$206 \quad \Delta Q = \Delta Q_{clim} + \Delta Q_{lulc}$$

207 Then, the contribution of landcover/landuse ($\% \Delta Q$) can be estimated as:

$$208 \quad \% \Delta Q_{lulc} = (\Delta Q - \Delta Q_{clim}) / \Delta Q * 100, \text{ or } \% \Delta Q_{lulc} = (1 - \Delta Q_{clim} / \Delta Q) * 100$$

$$209 \quad \Delta Q = \text{observed mean annual } Q \text{ in the second period} - Q \text{ in reference period (i.e., } \bar{Q}_0)$$

210 We used the Climate Elasticity Model (CEM) and the Rainfall-Runoff model (RRM) to determine
 211 ΔQ_{clim} (Li et al., 2007). The CEM involved developing an empirical relationship between deviation
 212 of Q (ΔQ_{0i}) and deviations P (ΔP_{0i}) and PET (ΔPET_{0i}) from the long-term means for the
 213 reference period:

$$\frac{\Delta Q_{0i}}{\bar{Q}_0} = \alpha \cdot \frac{\Delta P_{0i}}{\bar{P}_0} + \beta \cdot \frac{\Delta PET_{0i}}{\bar{PET}_0}$$

214 where, α and β were fitted ‘climate sensitivity’ parameters derived from annual climate data for the

215 reference period (1986-2002) in this study as determined by the double mass method while \bar{Q}_0
 216 and \bar{P}_0 were mean measured annual streamflow and precipitation. \overline{PET}_0 represents mean annual
 217 potential ET estimated by the FAO reference ET method (Allen et al., 1994). Then, the effects of
 218 the climate change in the second period in question could be calculated as:

$$\Delta\bar{Q}_{clim} = \bar{Q}_{pre} - \bar{Q}_0$$

219 where $\Delta\bar{Q}_{clim}$, \bar{Q}_{pre} , \bar{Q}_0 represents the mean effects of climate change on annual streamflow
 220 during the second period, predicted mean streamflow using the climate (P and PET) for the second
 221 period and the empirical equation developed from the reference period, and observed streamflow
 222 during the reference period, respectively.

223 The second method Rainfall-Runoff Model (RRM) was chosen to strengthen the attribution
 224 analysis by considering the seasonal climatic variability. This method involved developing the
 225 relationships between Q, P, and the variances (σ_{oi}^2) of P calculated using monthly P data series
 226 without consideration of PET (Jones et al, 2006; Li et al., 2007):

$$Q_{oi} = a + bP_{oi}(\sigma_{oi}^2)^c$$

227 Where Q_{oi} and P_{oi} is the annual Q and P for the reference period, respectively while σ_1^2 is the
 228 variance of the monthly P. The values of the three parameter, a , b , and c were derived using data
 229 from the reference period. The empirical model was then applied to estimate annual streamflow
 230 using precipitation for the second period (Q_{pre}) and finally to calculate the mean changes in Q
 231 ($\Delta\bar{Q}_{clim}$) as the differences between \bar{Q}_{pre} and mean streamflow for the reference period (\bar{Q}_0).

232 **3 Results**

233 **3.1 Land conversion and change in LAI**

234 During 2000-2012, the QRB has gone through dramatic land cover changes characterized by an
235 increase in urban areas and a decrease in paddy fields (Du et al., 2011, 2012; Chen and Du, 2014)
236 (see insert in Figure 2). The land cover change matrix showed that, from 2000 to 2012, the area of
237 urban built-up areas increased 388 km² or 174% at the expense of dry crop lands (decreased 43
238 km², or 6%), paddy fields (decreased 255 km², or 21%), and forest lands (decreased 83 km², or
239 23%) (Table 2). Since dryland changed relatively small from 2000 to 2012 (insert Figure 2 and
240 Table 2), majority of detected reduction in cropland area came from the changes in paddy fields.

241 MODIS data indicated that both mean annual and peak growing season watershed level LAI
242 decreased significantly ($p < 0.05$) with Z statistic = -2.08 and Z statistic = -2.41, respectively
243 (Table 3) (Figure 6). Since the major decrease in land use was paddy rice, the decline of LAI was
244 mainly caused by land conversion of paddy field to urban uses. The decrease trend of LAI
245 followed a similar pattern as ET during 2000-2013.

246 **3.2 Trend in Climate and MODIS ET**

247 The M-K test showed that the growing season precipitation had a weak increasing trend, but
248 annual total precipitation had an insignificant decreasing trend during 2000-2013 (Table 3). The
249 mean annual air temperature showed an insignificant change, but with a weak increase of 0.07°C
250 yr⁻¹ in the peak growing season from July to August (Table 3). Both annual and growing season
251 PET rose significantly by 7.5 mm yr⁻¹ (Z statistic = 2.5, $p < 0.05$) and 5.1 mm yr⁻¹ (Z statistic =
252 2.4, $p < 0.05$), respectively, an opposite trend of the actual ET (Table 3). The DHR method also
253 identified a rising trend for annual PET.

254 The mean annual MODIS ET was 655 mm yr⁻¹, varying from a low of 598 mm yr⁻¹ in 2011
255 to the highest 715 mm yr⁻¹ in 2002 during the study period (2000-2013). Annual ET exhibited a

256 general decreasing trend (-3.6 mm yr^{-1}) and pronounced decreases in the peak growing season of
257 July to August (-1.7 mm yr^{-1} , Z statistic = -2.3 , $p < 0.05$) (Table 3) (Figure 4). The ET linear trend
258 during the peak growing season (July-August) accounted for 32% of the total annual trend. Overall,
259 ET showed a similar decreasing trend with LAI in the peak growing season during 2000-2013
260 (Figure 6). Annual ET and the peak growing season ET departures from the long-term means had
261 significantly positive correlations with LAI departures ($R = 0.46$, $p = 0.1$; $R = 0.64$, $p = 0.015$,
262 respectively), but weak negative correlations with PET departures ($R = -0.38$, $p = 0.18$) during
263 2000-2013 (Figure 7).

264 **3.3 Changes in streamflow characteristics**

265 The FDC analysis for the flow measured at Wuding Sluice Gate indicated that both daily
266 highflows and lowflows were elevated during 2009-2013 compared to 2002-2008, with the median
267 flow rates increased from $30\text{m}^3\text{s}^{-1}$ to $38\text{m}^3\text{s}^{-1}$ (Figure 8). The extreme high flow in 2002-2008 was
268 caused by one extreme rainfall event in July, 2007 (rainfall = 339 mm) that resulted in widespread
269 flooding. The baseflow analysis also showed a significant ($p = 0$) increasing trend during
270 2006-2013 (Figure 9). The increase in baseflow or low flow coincided with the observations that
271 the groundwater levels in the study basin were on the rise in recent decade as a result of
272 groundwater management and likely landuse change in the recent decade (Figure 10). The runoff
273 coefficient (Streamflow/Precipitation ratio) during May-October period (wet, flooding seasons)
274 increased significantly from 0.32 to 0.41, or 28%, during 2002-2013 (Z statistic = 2.89 , $p < 0.01$)
275 (See insert in Figure 8).

276 **3.4 Changes in Annual Watershed Water Balances**

277 The DMC analysis identified a clear 'break point' of total annual streamflow (Q) around 2003

278 (Figure 11). The slopes of the regression lines between accumulated precipitation and streamflow
279 increased from 0.27 to 0.50. Mean annual streamflow significantly increased from 353 mm to 556
280 mm from period 1 (1986-2002) to period 2 (2003-2013) (Figure 12). This represented an increase
281 of runoff coefficient (Q/P) from 0.32 to 0.49, a 53% increase. The trend of annual streamflow was
282 influenced heavily by year 1991, a huge flooding event occurred in the Yangtze River Basin.
283 When this year was removed, R^2 increased from 0.1 to 0.34 and p value increased to a highly
284 significant level ($p = 0.002$). In the meantime, annual ET as estimated by P-Q, decreased
285 significantly from 752 mm to 578 mm from period 1 to period 2, representing a decline in ET by
286 23% or ET/P ratio by 25%.

287

288 **3.5. Contributions of LULC change and climate change and variability**

289 The two models gave consistent results on the contributions of climate change ($\% \Delta Q_{clim}$) and
290 LULC change ($\% \Delta Q_{lulc}$) to the observed annual increase (203 mm) in streamflow from the
291 reference period of 1986-2002 to the evaluation period 2003-2013 (Table 4). The CEM model
292 results suggested that the combinations of P and PET caused a decrease of streamflow and the
293 contribution of climate was negative (-8%). Thus the contribution of LULC was positive (108%),
294 more than 100%. In contrast, the RR model that did not include PET as a climatic factor suggested
295 P alone contributed 18% to the increase of streamflow while LULC change contributed 82%.

296 The modeling results indicate that PET is an important factor in evaluating the impacts of climate
297 and LULC change. Hydrologic change in the study basin was controlled by both precipitation and
298 PET. It appears that the effects of PET on streamflow (reducing flow) exceeded the influence of P
299 (increasing flow). Without considering the long-term change in air temperature, the contribution of

300 LULC might have been underestimated in this study.

301 **4 Discussion**

302 **4.1 Increased streamflow explained by the decreases in ET and LAI**

303 The total streamflow (Figure 12, Table 4), highflows, and lowflows (Figures 8, 9) in the QRB
304 have substantially increased during 2000-2013 while both LAI and ET have decreased (Figure 6,
305 Figure 12). Based on the watershed balance theory and comprehensive analyses using different
306 method including FDC, CEM, RRM, we attributed the dramatic increase in streamflow mainly to
307 the changes in LULC and associated decrease in LAI, not climate (PET or P), for the following
308 three complementary reasons.

309 First, LAI is a major controlling factor for ET, especially during the growing season (Sun et al.,
310 2011a, 2011b; Sun and Lockaby, 2012) and in humid, energy-limited southern China in particular
311 (Liu et al., 2013). The strong relationship between MODIS ET and LAI (Figures 6, Figure 7)
312 supported our hypothesis that urbanization dramatically reduced ET due to the reduction of LAI,
313 thus explained the observed increase in streamflow.

314 Second, regional annual ET is generally controlled by PET, P, and land surface conditions (Sun
315 et al., 2005). A decrease in ET is normally caused by a decrease in P and/or PET (Sun et al., 2005;
316 Sun et al., 2011a, 2011b). Our data suggested that the decrease in ET was not caused by PET or P
317 because annual and growing season PET significantly increased and overall precipitation did not
318 change significantly. In fact, a negative correlation was found between ET and PET departures
319 (Figure 7). The DMC method that eliminated precipitation effects on streamflow suggested the
320 QRB had a shift of annual streamflow upward around 2003 (Figure 11). The two models for

321 climate attribution analysis converged indicating that LULC contributed about 85% of the observed
322 variability in streamflow and precipitation contributed about 15%. PET increased more
323 dramatically during 2003-2013 than during 1986-2002 (Figure 12). The increase in PET might
324 have masked the decrease of ET due to change in LULC, so we argue that the estimated 85%
325 contribution from LULC is a conservative estimate.

326 Third, the large decrease in LAI as detected by remote sensing corresponded closely to the
327 dramatic conversion of rice paddy fields and increase in total impervious area (TIA) during the
328 urbanization campaign in the QRB since the early 2000s. Previous studies in the United States
329 suggest that stream flow and water quality regimes are degraded when the TIA exceeds 10-20% of
330 total watershed area (Arnold and Gibbons, 1996; Bledsoe and Watson, 2001). Our study result was
331 consistent with the finding of the threshold response in the literature, perhaps in the lower end of
332 the spectrum (<10%). The detected decrease in LAI due to shrinking rice paddy areas has
333 overwhelmed the impacts of climate change (i.e. rise of PET) on ET, highlighting the importance
334 of LULC change in evaluating environmental change in the study region.

335 **4.2 Regional hydrologic and environmental implications**

336 Our findings complement findings from an earlier study for the same basin. Du et al. (2011, 2012)
337 conducted a simulation study suggesting that the elevated highflow were mostly due to an increase
338 in impervious surface area. Our new analysis suggested that in addition to the increase in
339 impervious surface areas other factors such as reduced ET could be the main causes that
340 contributed to the observed increase in total flow and baseflow in the study basin. The present
341 study advanced the understanding of the processes of hydrologic disturbances. Study results had
342 important hydrological and environmental implications for paddy field-dominated regions in

343 China and elsewhere in East Asia.

344 First, we confirmed our hypothesis that converting water stress- free paddy fields to relatively
345 'dry' urban uses or impervious surfaces dramatically reduced ET (Figure 1). Thus, converting
346 wetlands, such as paddy fields, to impervious or built-up areas is expected to have a much higher
347 magnitude of hydrologic impacts than that for converting dry croplands or forests to urban land
348 uses (Tsai's, 2002; Boggs and Sun, 2011). The ET estimates based on two independent methods,
349 watershed water balance and remote sensing, all showed large decreases in ET.

350 Second, the populated study region is prone to floods and droughts due to the nature of a
351 strong summer monsoon climate (Gu et al., 2011). Urbanization is likely to exacerbate the flood
352 risks during the monsoon season as a result of decreased ET, an increased impervious surface area,
353 and decreased retention capacity (Kang et al., 1998; Kim et al., 2014). In addition, an increase in
354 stormflow has important concerns on stream channel stability, soil erosion, and reactivation of
355 streambed sediment and pollutants (Sun and Locakby, 2012). This is of particular concern given
356 the increasing trend of typhoon activities in southern China under climate change (Gu et al., 2011).

357 Third, the increasing trend in baseflow found in this study is in somewhat contradiction to the
358 popular literature that suggests otherwise (Ott and Uhlenbrook, 2004; Kim et al., 2005; Price et al.,
359 2011). We argue that the large reduction in ET from paddy fields might have overwhelmed the
360 reduction of groundwater recharge from the increased impervious surfaces. The QRB is still
361 dominated by croplands (62% of land area in 2012) and the dramatic reduction in water loss from
362 rice cultivation and irrigation needs likely elevated groundwater recharge from uplands or stream
363 channels overall (Figure 10). Other studies have shown that reductions in forest land coverage,
364 thus reduction in ET, could increase baseflow in the humid piedmont region in North Carolina

365 (Boggs and Sun, 2011) and northeastern U.S. (Lull and Sopper, 1969). Boggs and Sun (2011)
366 conclude that the effects of vegetation removal on streamflow are most pronounced during the
367 growing seasons when the contrast between ET from a vegetated surface and from an urbanized
368 surface is the highest. Therefore, it is plausible that replacing paddy fields with high ET with urban
369 land uses (e.g., lawns or impermeable surfaces) with low ET may result in similar effect as forest
370 removal during urbanization. Future studies should examine the seasonality of the trend of
371 baseflow change to confirm the effects of rice paddy conversion on baseflow and groundwater
372 change.

373 **4.3. Human factors affecting water balances**

374 The landscape and stream networks of the QRB have been altered for thousands of years by
375 humans. Our water balance analysis used a holistic approach to examine the natural rainfall-runoff
376 relationships at the watershed scale with minimum attention to human water supply and use within
377 the watershed. Currently, the QRB provides important ecosystem services such as drought/flood
378 prevention, crop irrigation, recreation, tourism, and emergency drinking water supply to the local
379 communities. Patterns of groundwater withdrawal from local acquirers and inter-basin transfers
380 are changing in the study basin as the speed of urbanization increases in the study region (Du et al.,
381 2012; Zhou et al., 2015). To meet the increasing demand on water supply and flood controls by the
382 urbanized communities, ponds, reservoirs, and drainage canals have been built. There are over 20
383 small reservoirs with the basin. These landuse patterns further undoubtedly have complicated the
384 quantification of water balances for a large basin (Hao et al., 2015) since each landuse change
385 factor might have affected different hydrologic components. Future studies should focus on
386 process-based understanding how land conversions affect the ET processes and this effect

387 manifests at the watershed in affecting stormflow and baseflow. In addition, inter-basin transfers
388 must be addressed to reduce potential water balance errors by full accounting water supply and use
389 within and across the QRB.

390 **5 Conclusions**

391 Using long term hydrometeorological records, land cover/land use change information, and remote
392 sensing-based biophysical and evapotranspiration data, this case study showed that streamflow
393 rates, both highflows and lowflows, in the Qinhuai River Basin have increased from 1986 to 2013.
394 A significant increase in streamflow and a decrease in ET in the study basin were detected, and the
395 changes were considered to be associated with urbanization characterized as shrinkage of rice
396 paddy fields and an increase in impervious surface area. Urbanization that resulted in a reduction
397 in LAI during the peak growing season overwhelmed the hydrological effects of climate warming
398 and precipitation variability during the study period. The importance of rice paddy fields in
399 regulating ET and hydrologic responses to disturbance has been underestimated in previous
400 similar studies. There is a research need to fully understand the ecohydrological processes that
401 control the effects of land conversions on land surface energy and water balances at multiple scales.
402 Models for assessing the ecosystem service function (e.g., climate cooling, flood retention) of rice
403 paddy fields must include proper algorithms describing the hydrological processes including ET
404 that links water and energy balances.

405 Rice cultivations have been practiced for thousands of years around the world. However,
406 converting rice paddy fields to other uses in southern China and East Asia has been on the rise
407 under a changing climate and demographics. Our study indicates that urbanization will likely

408 increase the risk of flooding, heat islands, and social vulnerability due to the loss of ecosystem
409 services of rice paddies. To minimize and mitigate the hydrologic and environmental impacts of
410 converting paddy fields down streams while maintaining resource sustainability requires an
411 integrated watershed management approach that involves careful urban planning (Dunne and
412 Leopold, 1978), landscape design (Dietz and Clausen, 2008), and irrigation management (Park et
413 al., 2009).

414

415 *Acknowledgements.* This study was supported by the Natural Science Foundation of China
416 (71373130), the Jiangsu Key Laboratory of Agricultural Meteorology Fund (No. KYQ1201), the
417 National Key Basic Research Program of China (2013CB430200, 2013CB430206), and IceMe of
418 NUIST. Partial support was from the Southern Research Station, USDA Forest Service.

419

420

421

422

423 **References**

- 424 Allen, R.G., Smith, M., Perrier, A., and Pereira, L. S.: An update for the definition of reference evapotranspiration,
425 ICID Bull., 43, 1-34, 1994.
- 426 Arnold, C.L., and Gibbons, C.J.: Impervious surface coverage: the emergence of a key environmental indicator, Am.
427 Planners Assoc. J., 62, 243-58, 1996.
- 428 Barron, O. V., Barr, A. D., and Donn, M. J.: Effect of urbanisation on the water balance of a catchment with shallow
429 groundwater, J. Hydrol., 485, 162-176, doi:10.1016/j.jhydrol.2012.04.027, 2013.
- 430 Bledsoe, B. P. and Watson, C. C.: Effects of urbanization on channel instability, J. Am. Water Resour. As., 37,
431 255-270, doi:10.1111/j.1752-1688.2001.tb00966.x, 2001.
- 432 Boggs, J. L. and Sun, G.: Urbanization alters watershed hydrology in the Piedmont of North Carolina, Ecohydrology,
433 4, 256-264, doi:10.1002/Eco.198, 2011.
- 434 Brath, A., Montanari, A., and Moretti, G.: Assessing the effect on flood frequency of land use change via hydrological
435 simulation (with uncertainty), J. Hydrol., 324, 141-153, doi:10.1016/j.jhydrol.2005.10.001, 2006.
- 436 Caldwell, P. V., Sun, G., McNulty, S. G., Cohen, E. C., and Myers, J. A. M.: Impacts of impervious cover, water
437 withdrawals, and climate change on river flows in the conterminous US, Hydrol. Earth Syst. Sc., 16,
438 2839-2857, doi: 10.5194/hess-16-2839-2012, 2012.
- 439 Chen, A. L., Du, J. K.: Simulation and forecast of land cover pattern in Qinhuai River Basin based on the CA- Markov
440 model, Remote Sens. Land Resour., 26(2): 184-189, doi:10.6046/gtzyyg.2014.02.29, 2014.
- 441 Dietz, M. E. and Clausen, J. C.: Stormwater runoff and export changes with development in a traditional and low
442 impact subdivision, J. Environ. Manage., 87, 560-566, doi:10.1016/j.jenvman.2007.03.026, 2008.
- 443 Du, J. K., Li, C., Rui, H., Li, Q., Zheng, D., Xu, Y. and Hu, S.: The change detection of impervious surface and its

444 impact on runoff in the Qinhuai River Basin, China, In:19th International Conference on Geoinformatics IEEE
445 pp1-5, 2011.

446 Du, J. K., Qian, L., Rui, H. Y., Zuo, T. H., Zheng, D. P., Xu, Y. P., and Xu, C. Y.: Assessing the effects of urbanization
447 on annual runoff and flood events using an integrated hydrological modeling system for Qinhuai River basin,
448 China, *J. Hydrol.*, 464, 127-139,doi:10.1016/j.jhydrol.2012.06.057, 2012.

449 Dunne, T. and Leopold, L.:*Water in environmental planning* (New York: W H Freeman and Company press), 1978.

450 Dow, C. L. and DeWalle, D. R.: Trends in evaporation and Bowen ratio on urbanizing watersheds in eastern United
451 States, *Water Resour. Res.*, 36, 1835-1843,doi:10.1029/2000wr900062, 2000.

452 Foley, J. A., DeFries, R., Asner, G. P., Barford, C., Bonan, G., Carpenter, S. R., Chapin, F. S., Coe, M. T., Daily, G. C.,
453 Gibbs, H. K., Helkowski, J. H., Holloway, T., Howard, E. A., Kucharik, C. J., Monfreda, C., Patz, J. A.,
454 Prentice, I. C., Ramankutty, N., and Snyder, P. K.: Global consequences of land use, *Science*, 309, 570-574,doi:
455 10.1126/science.1111772, 2005.

456 Gilbert, R. O.: *Statistical methods for environmental pollution monitoring* (New York: VanNostrand Reinhold press),
457 1987.

458 Gong, P., Wang, J., Yu, L., Zhao, Y.C., Zhao, Y.Y., Liang, L., Niu, Z.G., Huang, X.M., Fu, H.H., Liu, S., Li, C.C., Li,
459 X.Y., Fu, W., Liu, C.X., Xu, Y., Wang, X.Y., Cheng, Q., Hu, L.Y., Yao, W.B., Zhang, H., Zhu, P., Zhao, Z.Y.,
460 Zhang, H.Y., Zheng, Y.M., Ji, L.Y., Zhang, Y.W., Chen, H., Yan, A., Guo, J.H., Yu, L., Wang, L., Liu, X.J., Shi,
461 T.T., Zhu, M.H., Chen, Y.L., Yang, G.W., Tang, P., Xu, B., Ciri, C., Clinton, N., Zhu, Z.L., Chen, J., and Chen, J.:
462 Finer resolution observation and monitoring of global land cover: first mapping results with Landsat TM and
463 ETM+ data, *Int. J. Remote Sens.*, 34, 2607-2654, 2013.

464 Gu, C., Hu, L., Zhang, X., Wang, X., and Guo, J.: Climate change and urbanization in the Yangtze River Delta, *Habitat*
465 *Int.*,35,544-552, 2011.

466 Hao, L., Sun, G., Liu, Y. and Qian, H.: Integrated modeling of water supply and demand under management options
467 and climate change scenarios in Chifeng City, China. *J. Am. Water Resour. As.* 51, 655-671, DOI:
468 10.1111/1752-1688.12311, 2015.

469 He, B., Wang, Y., Takase, K., Mouri, G., and Razafindrabe, B. H. N.: Estimating Land Use Impacts on Regional Scale
470 Urban Water Balance and Groundwater Recharge, *Water Resour.Manag.*, 23, 1863-1873,doi:
471 10.1007/s11269-008-9357-2, 2009.

472 He, J. F., Liu, J. Y., Zhuang, D. F., Zhang, W., and Liu, M. L.: Assessing the effect of land use/land cover change on
473 the change of urban heat island intensity, *Theor. Appl. Climatol.*, 90, 217-226,doi:10.1007/s00704-006-0273-1,
474 2007.

475 Jacobson, C. R.: Identification and quantification of the hydrological impacts of imperviousness in urban catchments:
476 A review, *J. Environ.Manage.*, 92, 1438-1448, 2011.

477 Jones, R.N., Chiew, F.H.S., Boughton, W.C., and Zhang, L.: Estimating the sensitivity of mean annual runoff to
478 climate change using selected hydrological models. *Adv. Water Resour.*, 29, 1419-1429, doi:
479 10.1016/j.advwatres.2005.11.001, 2006.

480 Jonsson, P. and Eklundh, L.: TIMESAT - a program for analyzing time-series of satellite sensor data, *Comput.*
481 *Geosci-Uk*, 30, 833-845, 2004.

482 Kang, I. S., Park, J. I., and Singh, V. P.: Effect of urbanization on runoff characteristics of the On-Cheon stream
483 watershed in Pusan, Korea, *Hydrol. Process*, 12, 351-363, 1998.

484 Kendall, M. G.: *Rank correlation methods* London: Charles Griffin press, 1975.

485 Kim, S. J., Kwon, H. J., Park, G. A., and Lee, M. S.: Assessment of land-use impact on streamflow via a grid-based
486 modelling approach including paddy fields, *Hydrol. Process.*, 19, 3801-3817,doi:10.1002/Hyp.5982, 2005.

487 Kim, Y. J., Kim, H. D., and Jeon, J. H.: Characteristics of Water Budget Components in Paddy Rice Field under the

488 Asian Monsoon Climate: Application of HSPF-Paddy Model, *Water-Sui.*, 6, 2041-2055,
489 doi:10.3390/W6072041, 2014.

490 Li L-J, Zhang, L, Wang, H, Wang, J, Yang, J-W, Jiang, D-J, Li, J-Y, and Qin, D-Y.: Assessing the impact of climate
491 variability and human activities on streamflow from the Wuding River basin in China, *Hydrol. Process.*, 21,
492 3485-3491, doi: 10.1002/hyp.6485, 2007.

493 Liu, Y., Zhou, Y., Ju, W., Chen, J., Wang, S., He, H., Wang, H., Guan, D., Zhao, F., Li, Y., and Hao, Y.:
494 Evapotranspiration and water yield over China's landmass from 2000 to 2010, *Hydrol. Earth Syst. Sci.*, 17,
495 4957-4980, doi:10.5194/hess-17-4957-2013, 2013.

496 Lull, H.W. and Sopper, W.E.: Hydrologic effects from urbanization of forested watersheds in the Northeast. USDA
497 Forest Service Research Paper NE-146. Northeastern Forest Experiment Station, 1969.

498 Ma, H. A., Yang, D. W., Tan, S. K., Gao, B., and Hu, Q. F.: Impact of climate variability and human activity on
499 streamflow decrease in the Miyun Reservoir catchment, *J. Hydrol.*, 389,
500 317-324, doi:10.1016/j.jhydrol.2010.06.010, 2010.

501 Mann, H. B.: Non-parametric test against trend, *Econometrica*, 13, 245-259, 1945.

502 McDonald, R. I., Green, P., Balk, D., Fekete, B. M., Revenga, C., Todd, M., and Montgomery, M.: Urban growth,
503 climate change, and freshwater availability, *P. Natl. Acad. Sci. USA*, 108, 6312-6317, doi:
504 10.1073/pnas.1011615108, 2011.

505 Miller, J. D., Kim, H., Kjeldsen, T. R., Packman, J., Grebby, S., and Dearden, R.: Assessing the impact of urbanization
506 on storm runoff in a pen-urban catchment using historical change in impervious cover, *J. Hydrol.*, 515,
507 59-70, doi:10.1016/j.jhydrol.2014.04.011, 2014.

508 Mu, Q. Z., Zhao, M. S., and Running, S. W.: Improvements to a MODIS global terrestrial evapotranspiration
509 algorithm, *Remote Sens. Environ.*, 115, 1781-1800, doi: 10.1016/j.rse.2011.02.019, 2011.

510 Ott, B. and Uhlenbrook, S.: Quantifying the impact of land-use changes at the event and seasonal time scale using a
511 process-oriented catchment model, *Hydrol. Earth Syst. Sc.*, 8, 62-78, 2004.

512 Paul, M. J. and Meyer, J. L.: Streams in the urban landscape, *Annu. Rev. Ecol. Syst.*, 32, 333-365, 2001.

513 Price, K., Jackson, C. R., Parker, A. J., Reitan, T., Dowd, J., and Cyterski, M.: Effects of watershed land use and
514 geomorphology on stream low flows during severe drought conditions in the southern Blue Ridge Mountains,
515 Georgia and North Carolina, United States, *Water Resour. Res.*, 47, W02516, doi:10.1029/2010wr009340, 2011.

516 Roderick, M. L., Hobbins, M. T., and Farquhar, G. D.: Pan evaporation trends and the terrestrial water balance. II.
517 Energy balance and interpretation, *Geogr. Compass*, 3, 761-780, 2009.

518 Sakaguchi, A., Eguchi, S., and Kasuya, M.: Examination of the water balance of irrigated paddy fields in SWAT 2009
519 using the curve number procedure and the pothole module, *Soil Sci. Plant Nutr.*, 60,
520 551-564, doi:10.1080/00380768.2014.919834, 2014.

521 Sun, G., McNulty, S. G., Lu, J., Amatya, D. M., Liang, Y., and Kolka, R. K.: Regional annual water yield from forest
522 lands and its response to potential deforestation across the southeastern United States, *J. Hydrol.*, 308,
523 258-268, doi: 10.1016/j.jhydrol.2004.11.021, 2005.

524 Sun, G., Alstad, K., Chen, J. Q., Chen, S. P., Ford, C. R., Lin, G. H., Liu, C. F., Lu, N., McNulty, S. G., Miao, H. X.,
525 Noormets, A., Vose, J. M., Wilske, B., Zeppel, M., Zhang, Y., and Zhang, Z. Q.: A general predictive model for
526 estimating monthly ecosystem evapotranspiration, *Ecohydrology*, 4, 245-255, doi: 10.1002/Eco.194, 2011a.

527 Sun, G., Caldwell, P., Noormets, A., McNulty, S. G., Cohen, E., Myers, J. M., Domec, J. C., Treasure, E., Mu, Q. Z.,
528 Xiao, J. F., John, R., and Chen, J. Q.: Upscaling key ecosystem functions across the conterminous United
529 States by a water-centric ecosystem model, *J. Geophys. Res-Bioge.*, 116, doi:10.1029/2010jg001573, 2011b.

530 Sun, G. and Lockaby, B.G.: Chapter 3: Water quantity and quality at the urban-rural interface. In: D N Laband, B G
531 Lockaby and W Zipperer (Eds). *Urban-Rural Interfaces: Linking People and Nature*. (ASACSS, SSAmerica,

532 Madison, WI) pp26-45, 2012.

533 Tang, L. H., Yang, D. W., Hu, H. P., and Gao, B.: Detecting the effect of land-use change on streamflow, sediment and
534 nutrient losses by distributed hydrological simulation, *J. Hydrol.*, 409,
535 172-182,doi:10.1016/j.jhydrol.2011.08.015, 2011.

536 Taylor, C. J., Pedregal, D. J., Young, P. C., and Tych, W.: Environmental time series analysis and forecasting with the
537 Captain toolbox, *Environ. Modell. Softw.*, 22, 797-814,doi: 10.1016/j.envsoft.2006.03.002, 2007.

538 Tsai, M. H.: The Multi-functional roles of paddy field irrigation in Taiwan,Proceedings of the pre-symposium for the
539 third world water forum (WWF3), 217-220, 2002.

540 Vogel, R. M. and Fennessey, N. M.: L-Moment Diagrams Should Replace Product Moment Diagrams, *Water Resour.*
541 *Res.*, 29, 1745-1752,1993.

542 Wahl, K. L. and Wahl, T. L.:Determining the flow of Comal Springs at New Braunfels, Texas, Texas Water
543 '95,American Society of Civil Engineers (San Antonio, Texas), pp77-86, August 16-17, 1995.

544 Wang, Y. J., Lv, H. J., Shi, Y. F., and Jiang, T.: Impacts of land use changes on hydrological processes in an
545 urbanized basin: a case study in the Qinhuai River Basin, *J. Nat. Resour.*, 24, 30-36, 2009.

546 Wei, X. H. and Zhang, M. F.: Quantifying streamflow change caused by forest disturbance at a large spatial scale: A
547 single watershed study, *Water Resour. Res.*, 46,W12525,doi: 10.1029/2010wr009250, 2010.

548 Wu, R.S., Sue, W.R.,and Chang, J.D.: A simulation model for investigating the effects of rice paddy fields on runoff
549 system In: Zenger A and Argent RM (eds) MODSIM97 International Congress on Modelling and Simulation.
550 Modelling and Simulation Society of Australia and New Zealand, pp 422-427, 1997.

551 Xiao, Y., An, K., Xie, G., and Lu, C.: Evaluation of Ecosystem Services Provided by 10 Typical Rice Paddies in
552 China, *J. Resour. Ecol.*, 2, 328-337, 2011.

553 Yang, L., Tian, F. Q., J. A. Smith, and Hu. H. P.: Urban Signatures in the Spatial Clustering of Summer Heavy
554 Rainfall Events over the Beijing Metropolitan Region, *J. Geophys. Res. Atmos.*, 119, 1203-1217,
555 doi:10.1002/2013JD020762, 2013.

556 Yuan, H., Dai, Y. J., Xiao, Z. Q., Ji, D. Y., and Shangguan, W.: Reprocessing the MODIS Leaf Area Index products for
557 land surface and climate modelling, *Remote Sens. Environ.*, 115, 1171-1187,doi: 10.1016/j.rse.2011.01.001,
558 2011.

559 Zhao, L., Lee, X., Smith, R. B., and Oleson, K.: Strong contributions of local background climate to urban heat islands,
560 *Nature*, 511, 216-219,doi: 10.1038/Nature13462, 2014.

561 Zhou, D, Zhao, S, Liu, S, Zhang, L, and Zhu C: Surface urban heat island in China's 32 major cities: Spatial patterns
562 and drivers. *Remote Sens. Environ.*, 152, 51-61, 2014.

563

564 **Table 1.** A summary of landuse, climate, and hydrology data resources

Data Type	Data resources	Data details	Periods	Spatio-temporal resolution
Land use / Land cover	Landsat TM and ETM+ images(http://glovis.usgs.gov/) Published thesis and journal papers (Du et al., 2012; Chen, Du, 2014; Gong et al., 2013)	Land use / Land cover types	1988,1994, 2000, 2004, 2007 and 2012	30 m
Climate	Jiangsu meteorological bureau (4 meteorological stations)	Precipitation, radiation, temperature, wind speed, and humidity	1961-2013	Daily,
Streamflow	Two hydrological stations: the Wuding Sluice Gate and the Inner Qinhuai Sluice Gate. Published journal papers (Du et al., 2011)	Streamflow	2002-2003 (May-October), 2006-2013 (May-October), 1986-2006	Daily (2002-2003, 2006-2013); Annual (1986-2006)
Groundwater	Aiyuan well station	Groundwater table depth	2006-2013	Monthly
Actual ET	Improved MOD16 datasets (Mu et al., 2011)	Actual ET	2000-2013	Eight-day and 1-km ² resolution
Leaf Area Index (LAI)	Improved MODIS LAI datasets(http://globalchange.bnu.edu.cn/research/lai) (Yuan et al.,2011)	LAI	2000-2013	Eight-day and 1-km ² resolution

565

566

567

568

570 **Table 2.** The conversion matrix for land use change during 2000-2012 in the Qinhuai River Basin.

2000 (km ²)	2012 (km ²)					Σ (2000)
	Dry crop lands	Paddy fields	Forest	Water	Urban built-up areas	
Dry crop lands	320	226	7	8	175	736
Paddy fields	257	681	6	24	220	1,188
Forest	74	2	264	2	24	366
Water	16	12	2	59	14	104
Urban built-up areas	26	13	3	3	178	223
Σ (2012)	693	933	283	96	611	2,617
Area change from 2000 to 2012	-43	-255	-83	-8	388	--
Area change from 2000 to 2012 (%)	-6	-21	-23	-8	174	--

573 **Table 3.** Summary of Z statistics by the Nonparametric Mann-Kendall trend tests for temperature
 574 (T), ET, PET, precipitation (P), and LAI during the periods of July-August, April-October, and
 575 annual, Qinhuai River Basin (2000-2013).

Periods	Z statistic				
	LAI(s)	ET(s) (mm)	PET(s) (mm)	P(s) (mm)	T(s) (°C)
July-August	-2.41 [*] (-0.04)	-2.3 [*] (-1.7)	1.3(2.4)	1.31(12.9)	1.31(0.07)
April-October	-2.30 [*] (-0.02)	-1.2(-2.4)	2.4 [*] (5.1)	0.11(2.6)	0.77(0.02)
Annual	-2.08 [*] (-0.01)	-1.5(-3.6)	2.5 [*] (7.5)	-0.55(-8.0)	0.00(-0.00)

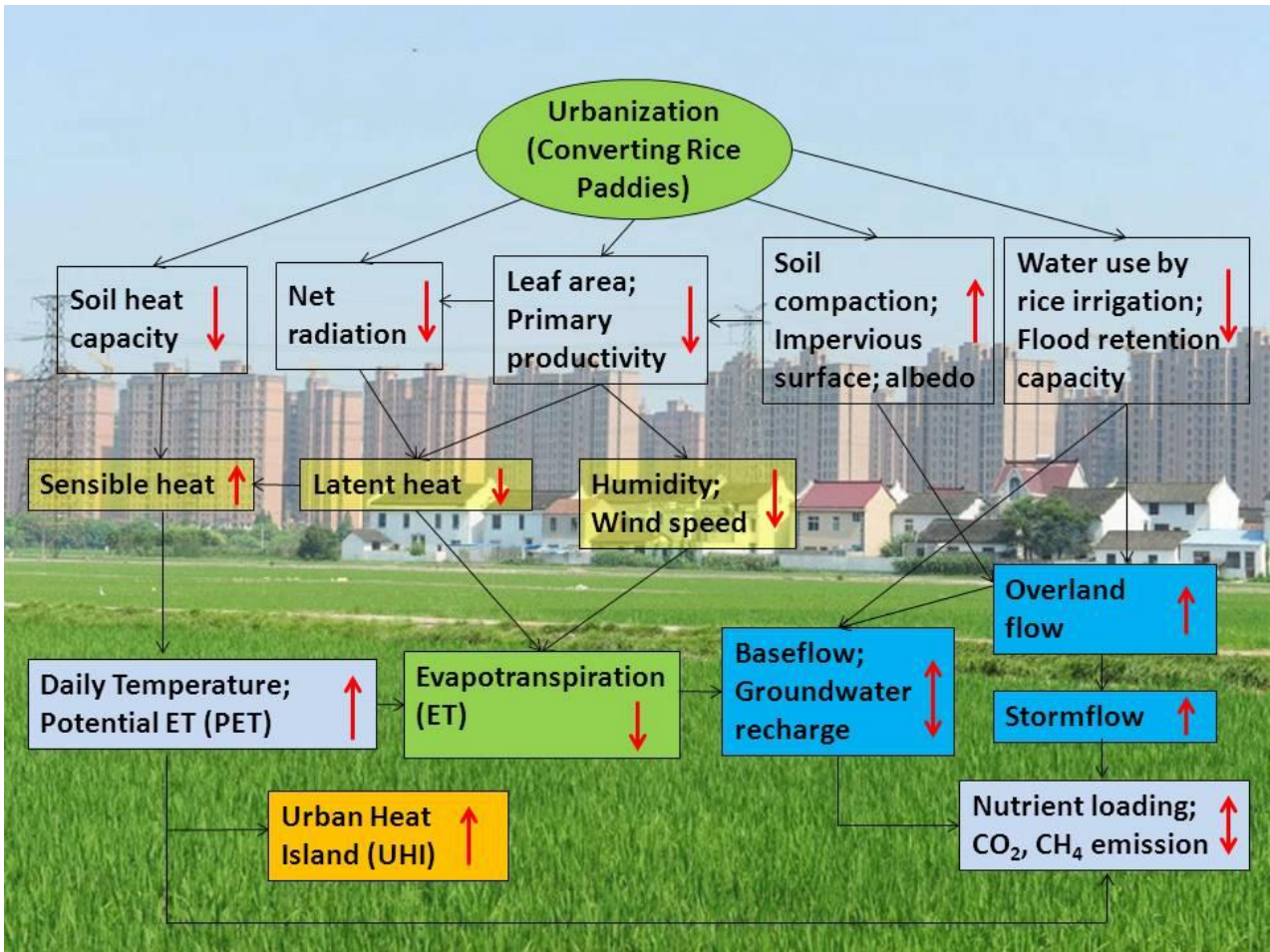
576 ^{*}Denotes significance level of 0.05. ‘s’ is the true slope of the linear trend, i.e., change per year.
 577

578 **Table 4.** Modeled contributions of land use change and climate change on the increase in
 579 streamflow (mm yr^{-1}) by the Climate Elasticity Model (CEM) and Rainfall Runoff Model (RRM).

Period	\bar{P}	\overline{PET}	\bar{Q}	ΔQ_o	CEM		RRM	
					$(\alpha=0.27; \beta=-0.65)$		$(a=-509; b=0.45; c=0.064)$	
					$\Delta\bar{Q}_{clim}$	$\Delta\bar{Q}_{lulc}$	$\Delta\bar{Q}_{clim}$	$\Delta\bar{Q}_{lulc}$
1986-2002 (reference)	1105±291	998±82	353±287	--				
2003-2013	1134±178	1075±45	556±145	203	-15 ± 23(-8%)	218±131(108%)	36 ± 169(18%)	167 ± 100(82%)

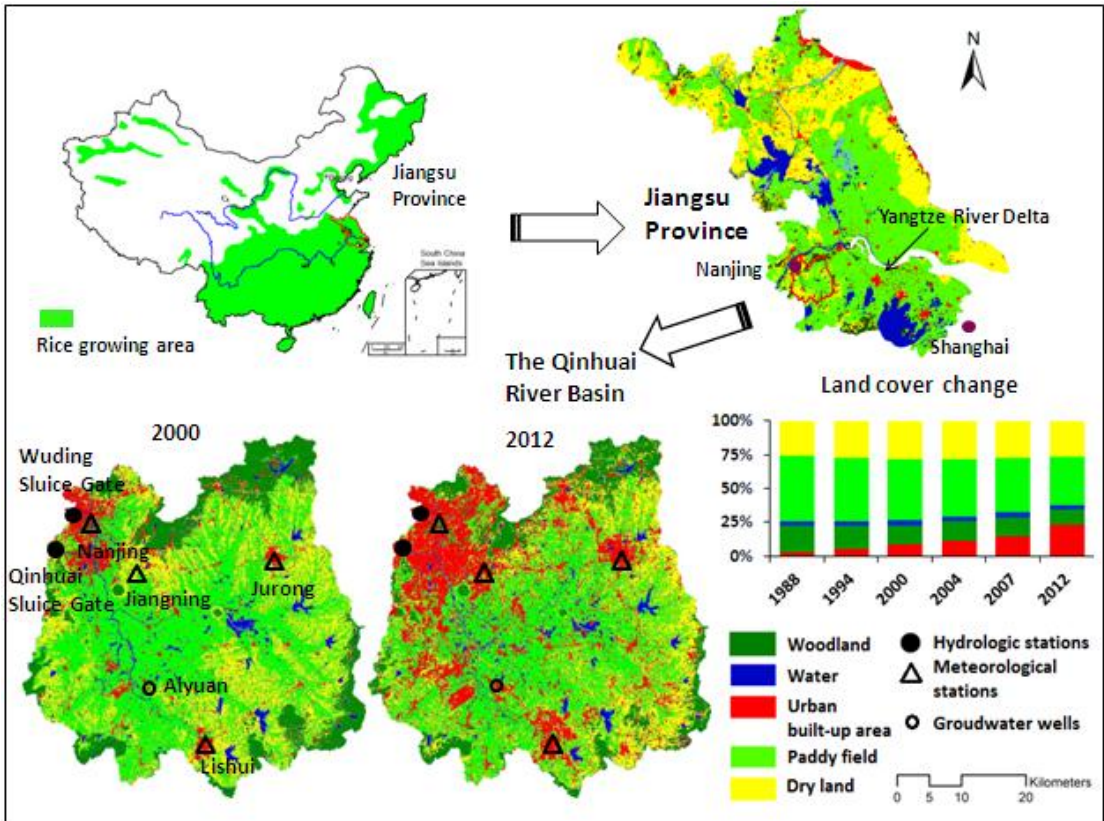
580
 581
 582
 583
 584
 585
 586
 587

588
589



590
591
592
593
594
595
596
597
598

Fig. 1. A conceptual model illustrating the potential hydrologic and environmental impacts of converting rice paddies to urban uses in the Yangtze River Delta region. Arrows represent directions (up or down or both) of change (Background photo credit: <http://blog.sciencenet.cn/blog-578415-712508.html>).



599

600 **Fig. 2.** Watershed location, instrumentation, and land use change patterns in the Qinhuai River
 601 Basin, Yangtze River Delta in southern China. The insert map showing changes in land use derived
 602 from published data (Du et al., 2012; Chen and Du, 2014) (1988 and 1994) and Landsat 7 ETM+
 603 images (2000-2012).

604

605

606

607

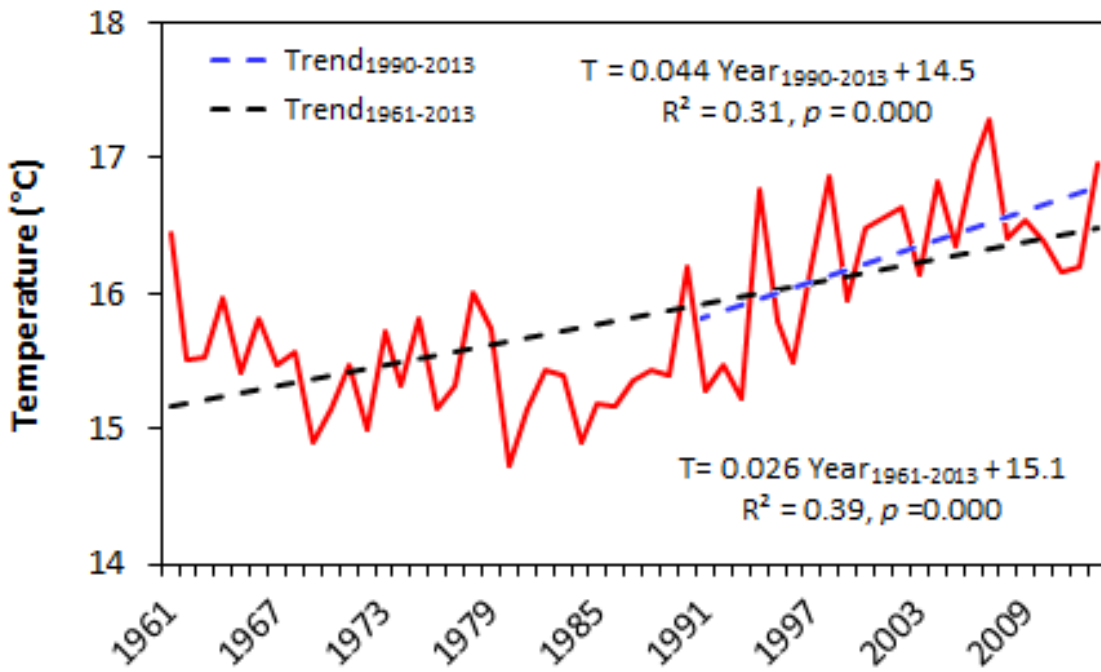
608

609

610

611

612



613

614 **Fig. 3.** Mean annual air temperature change across four meteorological stations in the Qinhuai
 615 River Basin in southern China during 1961-2013.

616

617

618

619

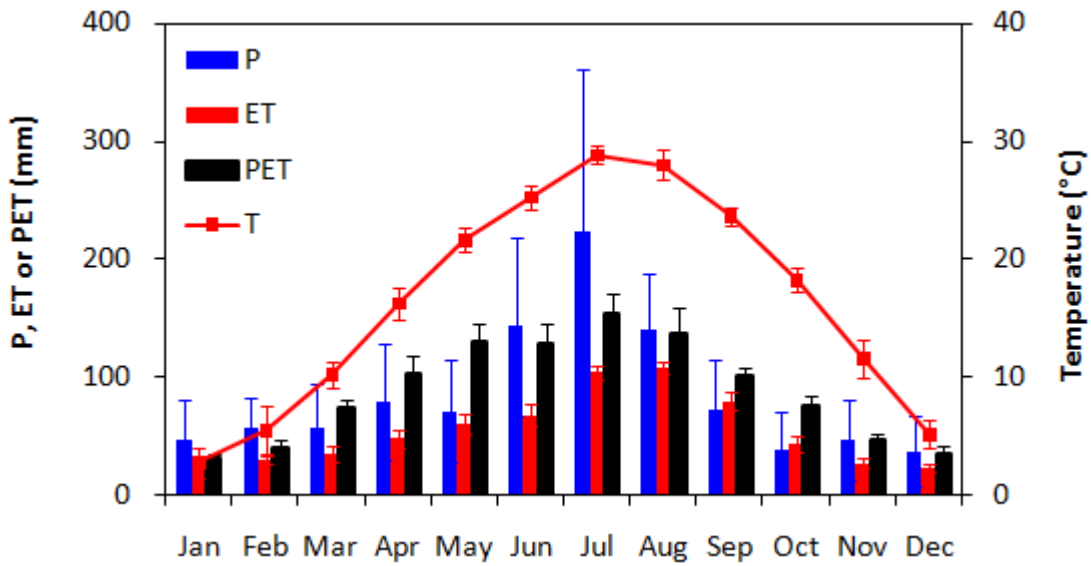
620

621

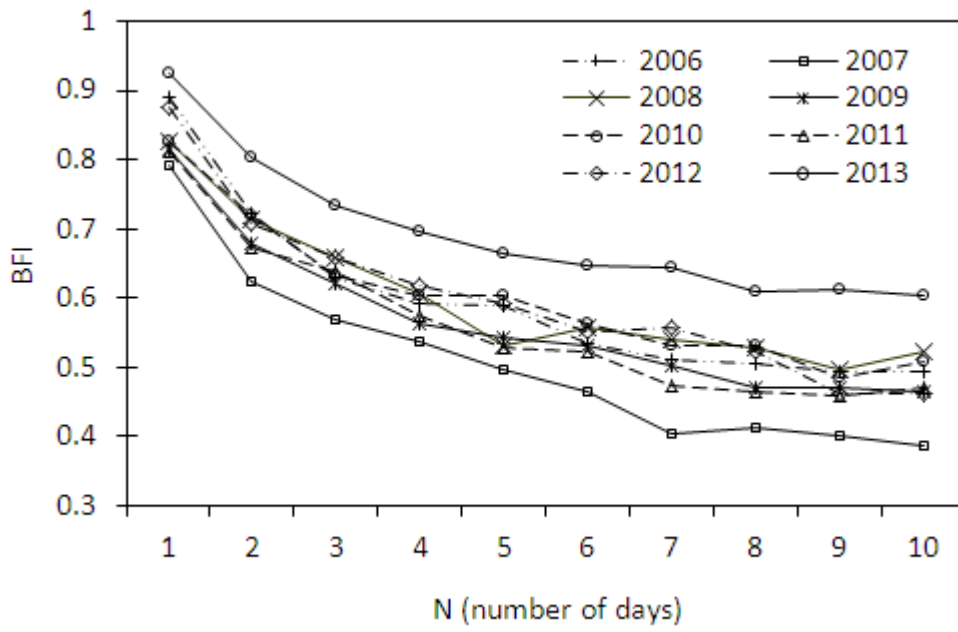
622

623

624



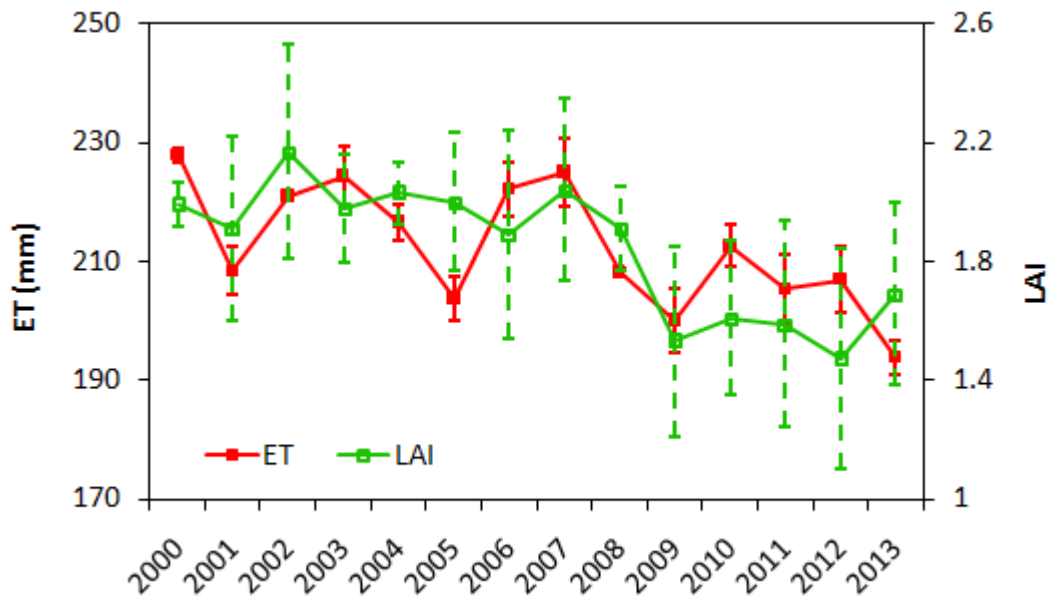
625 **Fig. 4.** Mean monthly precipitation (P) (1986-2013), MODIS evapotranspiration (ET) (2000-2013),
 626 potential evapotranspiration (PET) (2000-2013) and temperature (T) (1986-2013), and the vertical
 627 lines are standard deviation.
 628



629

630 **Fig. 5.** Sensitivity of Base-flow Index (BFI) to the number of days (N) used to select the minimum
 631 value in baseflow separation analysis from 2006 to 2013 at the Wuding Station located at the
 632 outlet of the Qinhuai River Basin.

633



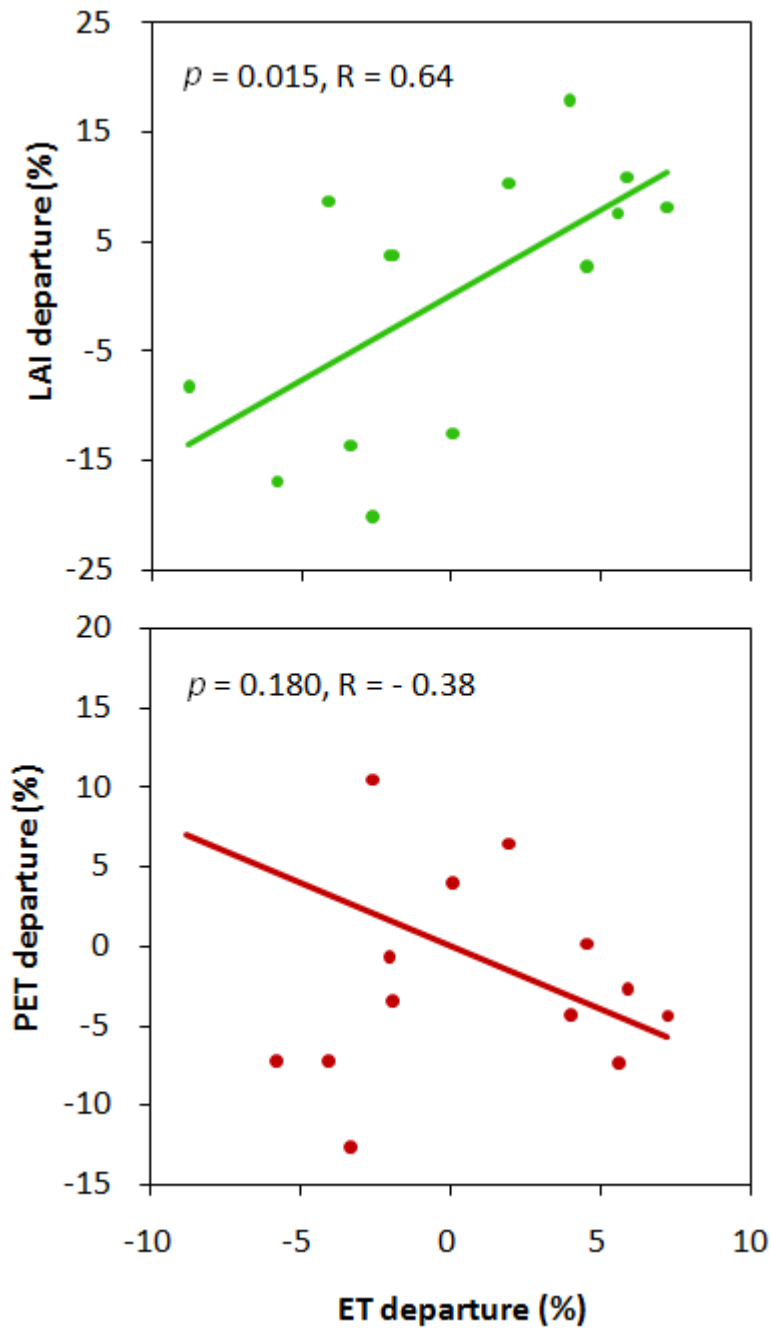
635

636 **Fig. 6.** Total MODIS ET (mm per two months) and mean LAI during the peak growing season

637 (July - August) over 2000-2013 in the Qinhuai River Basin. Vertical lines represent standard

638 deviation across space.

639



640

641 **Fig. 7.**Correlations of the departures of basin-level ET with (a) the departures of mean leaf area

642 index (LAI) and (b) the departures of PET in the peak growing season (July-August) over

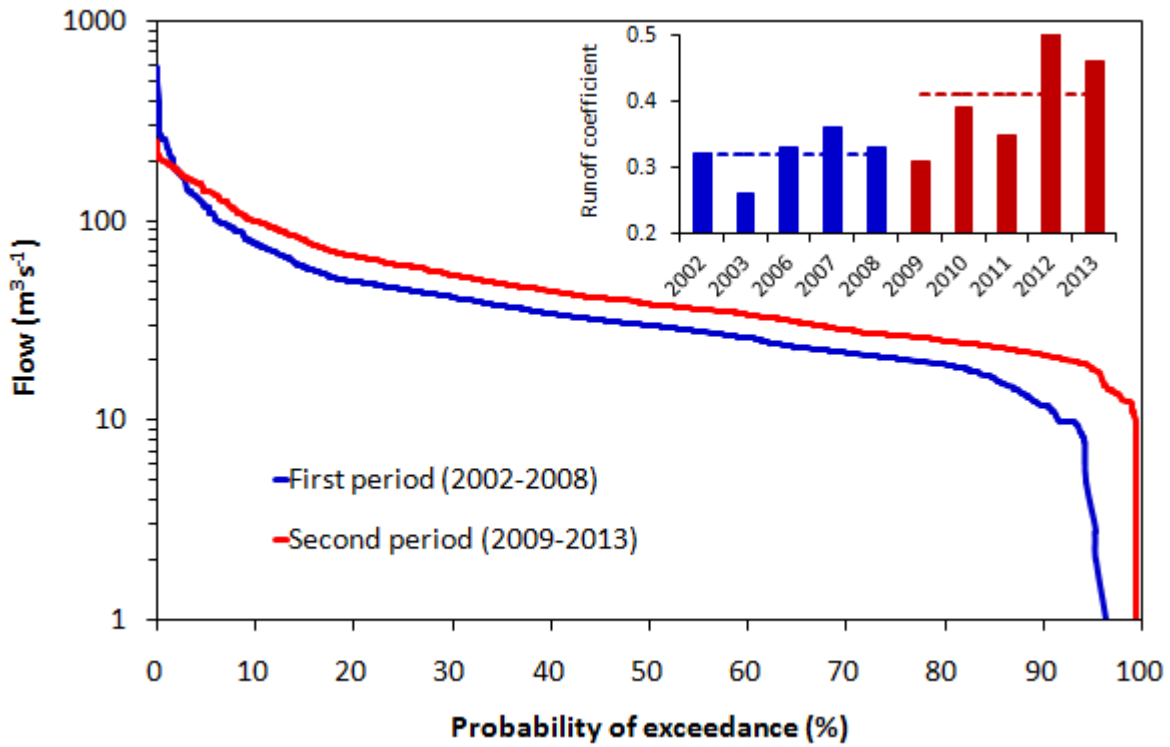
643 2000-2013 in the Qinhuai River Basin.

644

645

646

647



649

650 **Fig. 8.** Flow duration curves for mean daily flow in the first period (2002-2003 and 2006-2008)
 651 and the second period (2009-2013) (May-October) measured at the Wuding Station in the Qinhuai
 652 River Basin. Insert is runoff coefficient, the ratio of streamflow/precipitation for the period from
 653 May to October when the flow control gate was open.

654

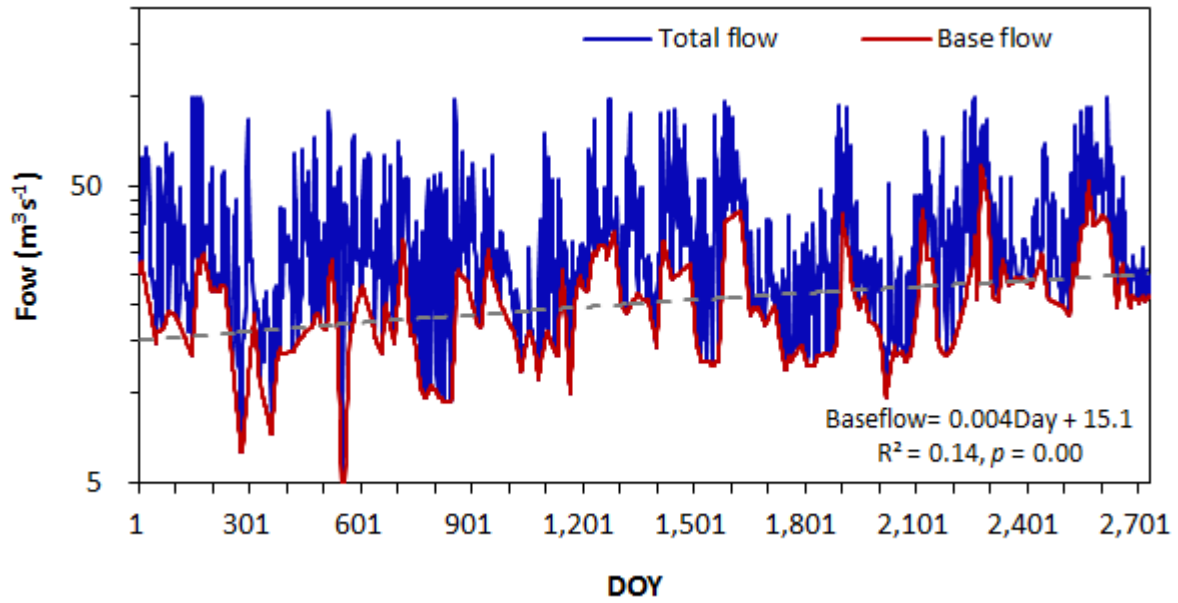
655

656

657

658

659

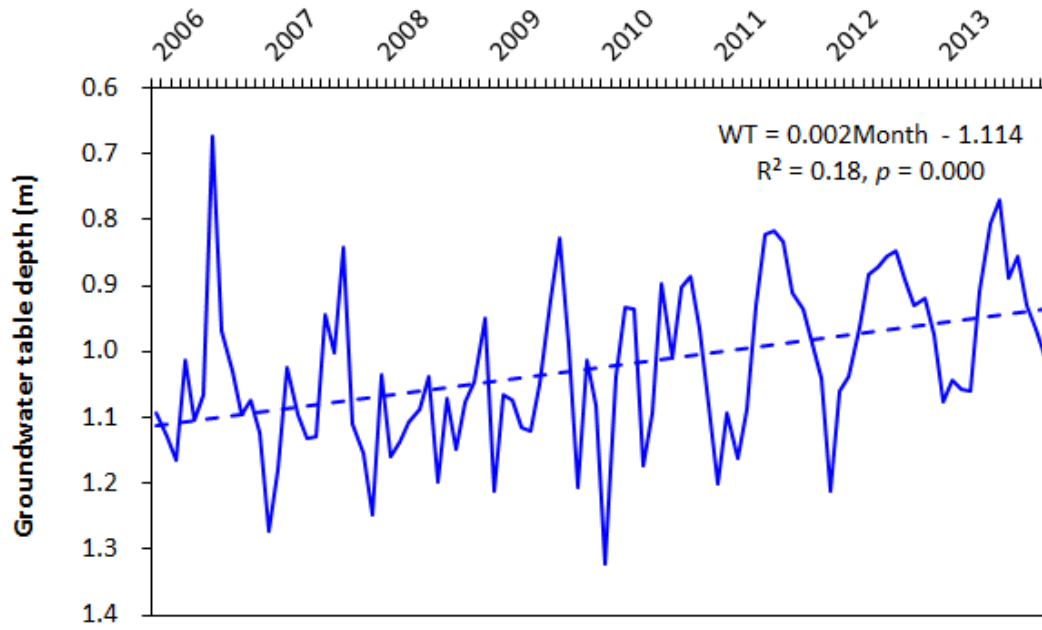


660

661 **Fig. 9.** Trend of daily base flow separated from total stream flow measured at the Wuding Station

662 during 2006-2013. DOY is the number of accumulated days since January 1, 2006.

663

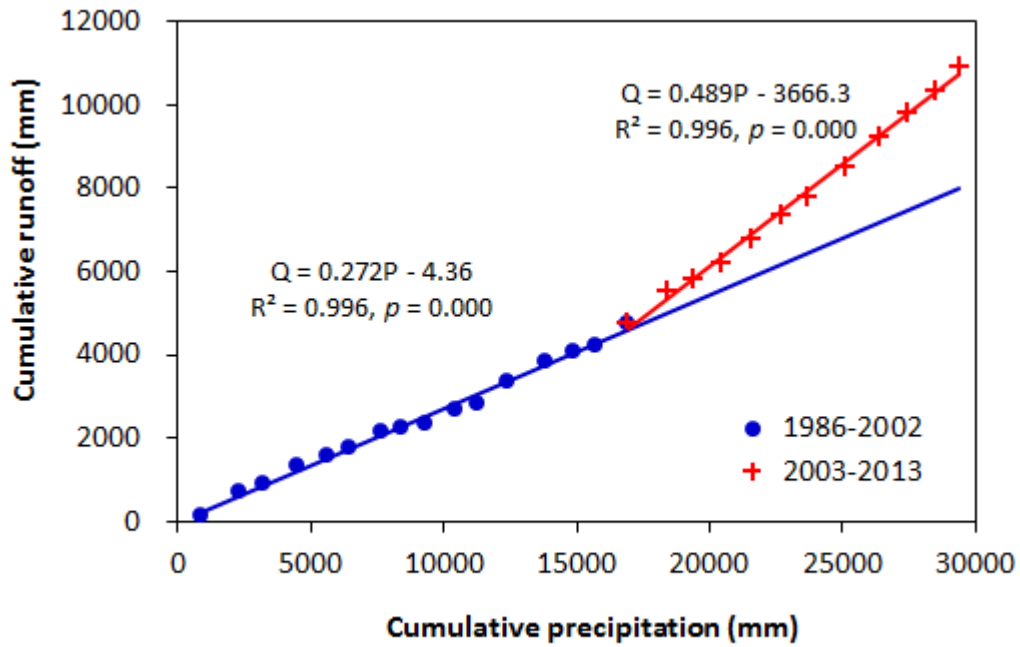


664

665 **Fig. 10.** The trend of monthly groundwater table depth fluctuations measured at the Aiyuan Well
666 Station in the Lishui sub basin during 2006-2013.

667

668

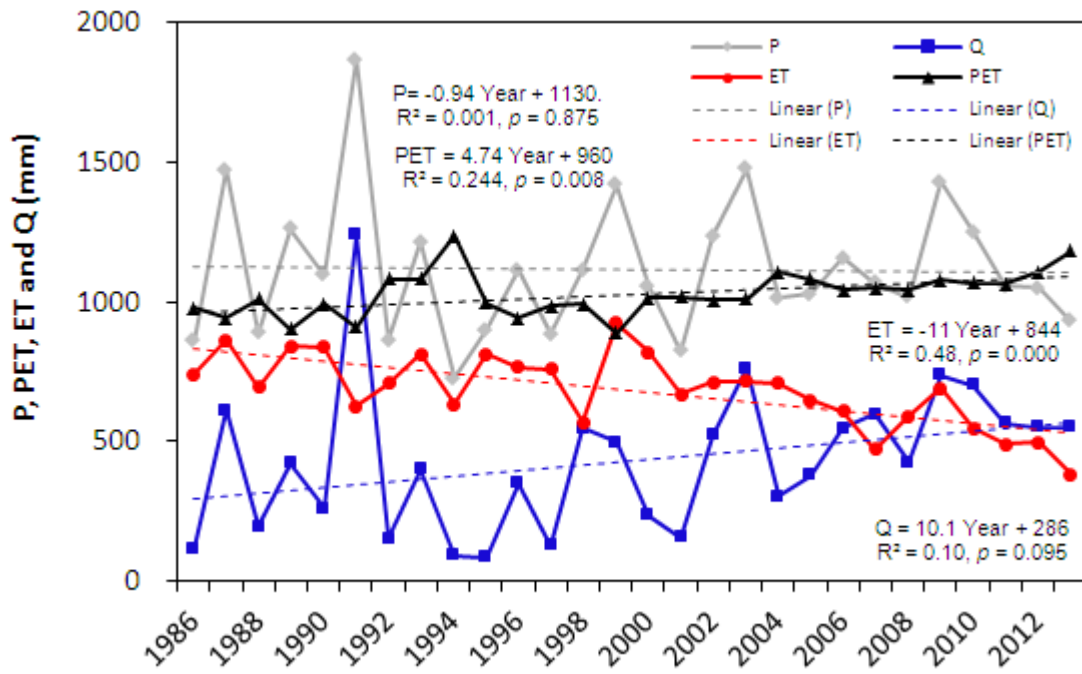


669

670 **Fig. 11.** Double mass curves showing the relationships between accumulated annual precipitation
 671 (P) and total streamflow (Q) for the Qinhuai River Basin (1986-2013). The extreme wet year of
 672 1991 was removed from the analysis.

673

674



675

676

677 **Fig. 12.** Trend of annual water balance and potential evapotranspiration (PET) for the Qinhuai

678 River Basin from 1986-2013. ET was estimated as the difference between precipitation (P) and

679 measured streamflow (Q).

680